Neutrino emissivity of the nucleon direct URCA process for rotational traditional and hyperonic neutron stars *

Nai-Bo Zhang(张乃波)[1] Shou-Yu Wang(王守宇)[1;1)] Bin Qi(亓斌)[1;2)]
Jian-Hua Gao(高建华)[1] Bao-Yuan Sun(孙保元)[2]

[1] Shandong Provincial Key Laboratory of Optical Astronomy and Solar-Terrestrial Environment, Institute of Space Sciences, Shandong University, Weihai 264209, China
[2] School of Nuclear Science and Technology, Lanzhou University, Lanzhou 730000, China

Abstract: Based on covariant density functional theory, we study the effects of rotation on the nucleon direct URCA (N-DURCA) process for traditional and hyperonic neutron stars. The calculated results indicate that, for a fixed mass sequence of rotational traditional neutron stars, the neutrino emissivity of the star is nearly invariant with increasing frequency, while it always increases for rotational hyperonic neutron stars. Thus, rotation has different effects on the N-DURCA process for these two kinds of neutron stars.

Keywords: neutron stars, hyperon, rotation, direct URCA process

PACS: 21.60.Jz, 26.60.-c, 97.60.Jd **DOI:** 10.1088/1674-1137/41/7/075101

1 Introduction

Neutron stars have particularly high internal temperatures ($10^{11}-10^{12}$ K) when they are born in supernova explosions. Their temperature then decreases to less than 10^{10} K within minutes [1]. The long-term cooling of neutron stars involves neutrino emission from the interior and photon emission from the surface. Neutrino emission dominates for about 10^5 years, until the surface temperature is less than 10^6 K [2]. Up to now, all the observed isolated cooling neutron stars whose thermal surface radiation has been detected are dominated by neutrino emission [3].

To understand the neutrino emission of cooling neutron stars, several neutrino emitting processes have been proposed in previous studies [4, 5]. Among all the processes, the simplest and most effective neutrino emitting process is the direct URCA process:

$$\mathrm{B_1 \rightarrow B_2 + l + \bar{\nu}_l, \quad B_2 + l \rightarrow B_1 + \nu_l,} \tag{1}$$

where $\mathrm{B_1}$ and $\mathrm{B_2}$ are baryons (nuclei or hyperons), and l is a lepton (electron or muon). Accordingly, the direct URCA process can be divided into the nucleon direct URCA (N-DURCA) and hyperon direct URCA (Y-DURCA) processes. The N-DURCA process can be written as:

$$\mathrm{n \rightarrow p + l + \bar{\nu}_l, \quad p + l \rightarrow n + \nu_l.} \tag{2}$$

If l is an electron (muon), it corresponds to the electron (muon) N-DURCA process. Considering the momentum conservation and charge neutrality condition, Ref. [2] pointed out that the N-DURCA process can take place if the proton fraction is larger than a critical value (x_{DU}) in the range 11.1%–14.8%.

When the density is larger than 2–3 times the saturation density, hyperons appear in the neutron stars [6]. References [7–11] have studied the effects of hyperons on the N-DURCA process and suggested that the existence of hyperons can reduce the neutrino emissivity of the N-DURCA process. The hyperon direct URCA process also exists once the Λ hyperon appears [12]. Furthermore, the superfluidity of hyperons can also affect the cooling of neutron stars [13–15]. In this paper, we focus on the simplest N-DURCA process. The more complicated hyperon direct URCA process will be discussed in future work.

It is well known that neutron stars are rotational. Rotation can change the properties of neutron stars, such as mass, radius, and so on. Reference [16] first discussed the effects of rotation on the N-DURCA process, using the MDI equation of state (EOS), which is constrained

Received 14 March 2017

* Supported by National Natural Science Foundation of China (11545011, 11405096), the Shandong Natural Science Foundation (ZR2014AQ012), the Young Scholars Program of Shandong University, Weihai (2015WHWLJH01) and the Fundamental Research Funds for the Central Universities (lzujbky-2016-30)

1) E-mail: sywang@sdu.edu.cn
2) E-mail: bqi@sdu.edu.cn

by the available data in relativistic heavy-ion collisions. They suggested that the proton fraction could drop below x_{DU} with the increase of frequency and thus make the N-DURCA process impossible. Reference [17] studied the same effects by employing the APR EOS, which uses the variational chain summation methods and the new Argonne ν_{18} two-nucleon interaction, and came to the same conclusion. Up to now, the N-DURCA process for rotational hyperonic neutron stars has not been discussed. The neutrino emissivity of the N-DURCA process for rotational neutron stars was not calculated in the previous studies.

Based on the above considerations, we have studied the effects of rotation on the N-DURCA process of traditional and hyperonic neutron stars. The baryon octet was fully considered in our calculations. The paper is organized as follows. Section 2 introduces the formalism used in the calculations. In Section 3, we show the effects of rotation on the N-DURCA process. Finally, a summary is given in Section 4.

2 Formalism

There are many relativistic theories used to study neutron stars. However, as far as we know, the baryon octet has been fully considered in only four theories, namely, relativistic mean-field (RMF) theory [18–21], quantum hadrodynamics [22], quark meson coupling (QMC) [23] and quark mean field theory [24] . These four theories can be divided into two kinds: (1) the RMF and quantum hadrodynamics theories consider that the baryons interact via the exchange of mesons; and (2) the QMC and quark mean field theories consider the internal structure of baryons based on the quark degree of freedom. In the present work, we choose one representative theory from each kind, i.e., the RMF and QMC theories.

The RMF theory adopts the relativistic Hartree approach with the no-sea approximation. With a limited number of free parameters, including the meson masses and meson-nucleon coupling constants, the RMF theory has achieved great success in the description of nuclear matter and finite nuclei in the past several decades [18, 19]. The RMF theory has also been used to study neutron stars and obtained a lot of valuable results [20, 25–32]. The starting point of the RMF theory is an effective Lagrangian density which considers two isoscalar mesons (σ and ω) and one isovector meson (ρ). The effective Lagrangian density for neutron stars is:

$$\begin{aligned}\mathcal{L} = &\sum_{\mathrm{B}}\overline{\psi}_{\mathrm{B}}[\mathrm{i}\gamma^{\mu}\partial_{\mu}-m_{\mathrm{B}}-g_{\sigma\mathrm{B}}\sigma-g_{\omega\mathrm{B}}\gamma^{\mu}\omega_{\mu}-g_{\rho\mathrm{B}}\gamma^{\mu}\tau_{\mathrm{B}}\cdot\rho_{\mu}\\&-e\gamma^{\mu}A_{\mu}\frac{1-\tau_{3\mathrm{B}}}{2}]\psi_{\mathrm{B}}+\frac{1}{2}\partial_{\mu}\sigma\partial^{\mu}\sigma-\frac{1}{2}m_{\sigma}^{2}\sigma^{2}-U(\sigma)\\&+\sum_{\lambda=\mathrm{e}^{-},\mu^{-}}\overline{\psi}_{\lambda}(\mathrm{i}\gamma^{\mu}\partial_{\mu}-m_{\lambda})\psi_{\lambda}-\frac{1}{4}\omega_{\mu\nu}\omega^{\mu\nu}+\frac{1}{2}m_{\omega}^{2}\omega_{\mu}\omega^{\mu}\\&+U(\omega)-\frac{1}{4}\rho_{\mu\nu}\rho^{\mu\nu}+\frac{1}{2}m_{\rho}^{2}\rho_{\mu}\rho^{\mu}.\end{aligned} \tag{3}$$

The specific meanings of each parameter can be found in Ref. [20].

On the other hand, the recent developed chiral quark - meson coupling (CQMC) model has been used to simulate neutron stars [23, 33]. In this model, the properties of nuclear matter can be self-consistently calculated by the coupling of scalar and vector fields to the quarks within nucleons [34, 35], and the quark - quark hyperfine structures due to the exchanges of gluons and pions are included based on chiral symmetry [36–38]. The Lagrangian density of the CQMC theory for neutron stars is shown below. It is similar to that of RMF theory but an additional π meson field is needed:

$$\begin{aligned}\mathcal{L} = &\sum_{\mathrm{B}}\overline{\psi}_{\mathrm{B}}(\mathrm{i}\gamma_{\mu}\partial^{\mu}-m_{\mathrm{B}})\psi_{\mathrm{B}}+\frac{1}{2}(\partial_{\mu}\sigma\partial^{\mu}\sigma-m_{\sigma}^{2}\sigma^{2})\\&+\frac{1}{2}m_{\omega}^{2}\omega_{\mu}\omega^{\mu}-\frac{1}{4}W_{\mu\nu}W^{\mu\nu}+\frac{1}{2}m_{\rho}^{2}\rho_{\mu}\cdot\rho^{\mu}\\&-\frac{1}{4}\boldsymbol{R}_{\mu\nu}\cdot\boldsymbol{R}^{\mu\nu}+\frac{1}{2}(\partial_{\mu}\pi\cdot\partial^{\mu}\pi-m_{\pi}^{2}\pi^{2})\\&+\sum_{\mathrm{B}}\overline{\psi}_{\mathrm{B}}[g_{\sigma\mathrm{B}}(\sigma)\sigma-g_{\omega\mathrm{B}}\gamma_{\mu}\omega^{\mu}+\frac{f_{\omega\mathrm{B}}}{2\mathcal{M}}\sigma_{\mu\nu}\partial^{\nu}\rho^{\mu}\cdot\boldsymbol{I}_{\mathrm{B}}\\&-\frac{f_{\pi\mathrm{B}}}{m_{\pi}}\gamma_{5}\gamma_{\mu}\partial^{\mu}\pi\cdot\boldsymbol{I}_{\mathrm{B}}]\psi_{\mathrm{B}}\\&+\sum_{\lambda=\mathrm{e}^{-},\mu^{-}}\overline{\psi}_{\lambda}(\mathrm{i}\gamma^{\mu}\partial_{\mu}-m_{\lambda})\psi_{\lambda}.\end{aligned} \tag{4}$$

Based on RMF theory, we adopted four EOSs to simulate neutron stars, namely, GL97 [39], PK1 [40], PKDD [40], and TM1 [41]. In addition, the MYN [23] and MCS [33] EOSs from CQMC theory are also adopted to compare with the RMF EOSs. The calculated EOSs are given in Fig. 1. The corresponding effective interactions with hyperons are denoted by adding "H", e.g.,

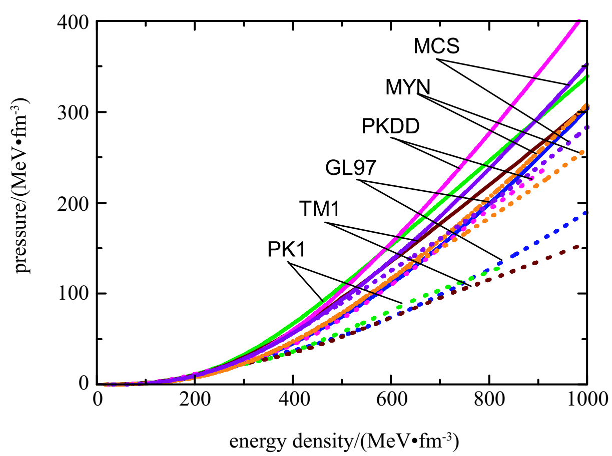

Fig. 1. (color online) The equations of state for neutron stars from RMF and CQMC theory without (solid lines) and with (dotted lines) hyperons.

GL97H. The meson-hyperons coupling constants and meson-nucleons coupling constants were fixed based on Ref. [42] for RMF EOSs, Ref. [23] for MYN EOS, and Ref. [33] for MCS EOS. The EOSs of the neutron star crust were replaced by the Negele and Vautherin EOS [43] and Baym-Pethick-Sutherland EOSs [44] for the inner and outer crust, respectively. As shown in Fig. 1, the EOSs without (solid lines) and with (dotted lines) hyperons are the same at low densities. However, the EOSs with hyperons are apparently softer than those without hyperons at high densities.

To show the compositions of the neutron stars, we present the particle fraction ($X_{\rm i} = n_{\rm i}/n_{\rm B}$) as a function of particle density (ρ) for PK1, PKDD, MYN and MSC EOSs without (a) and with (b) hyperons in Fig. 2. We can see from Fig. 2(a) that the compositions of all the EOSs exhibit the same tendency and only the fractions are a little different. However, as shown in Fig. 2(b), Σ^- is the first hyperon appearing at 0.23 (0.22) fm^{-3} for PKDD (PK1) EOS. More positive protons are needed to satisfy charge neutrality. On the other hand, only Ξ^- appears at 0.57 fm^{-3} in neutron stars for the MYN EOS, although the baryon octet is considered. This is because the Fock contribution enhances the repulsive effect mainly through ω mesons at supra-nuclear densities but the creation of Ξ^- is promoted by the inclusion of the tensor coupling with ρ mesons [45, 46]. Similarly, only Λ and Σ^- appear for the MCS EOS. It can be clearly seen that the particle types and fractions for the two kinds of EOSs shown here are quite different.

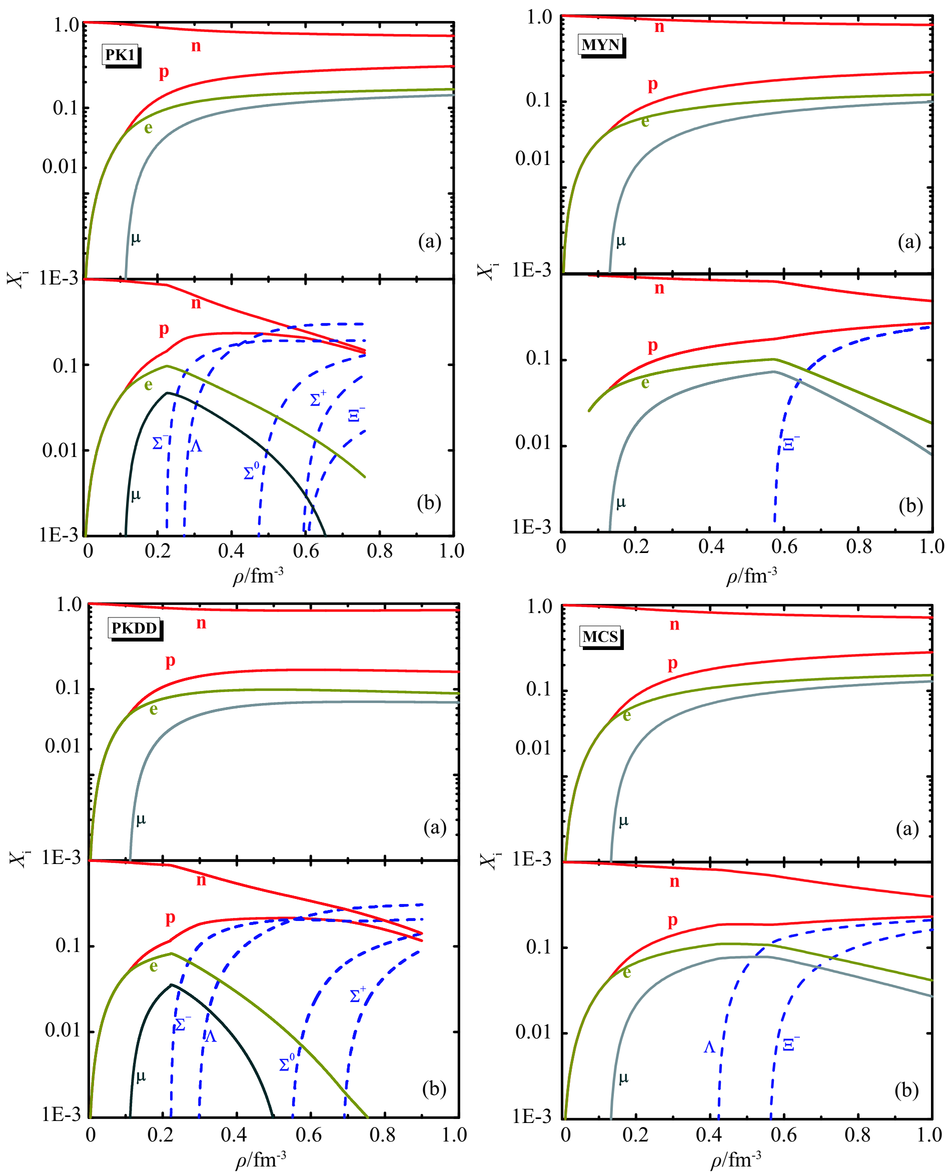

Fig. 2. (color online) The particle fraction ($X_{\rm i} = n_{\rm i}/n_{\rm B}$) as a function of the particle density (ρ) for PK1, PKDD, MYN, and MCS EOSs without (a) and with (b) hyperons. Each particle is labeled by its name.

Numerical calculations of rotational neutron stars have been performed using the RNS code (http://www.gravity.phys.uwm.edu/rns/). In the code, stationary configurations of rigidly rotational neutron stars are computed in the framework of general relativity by solving the Einstein equations for stationary axi-symmetric spacetime. More details about the code can be found in Ref. [47–51] and references therein.

To study the effects of hyperons and rotation on the N-DURCA process, we calculated the neutrino emissivity of the N-DURCA process. In Ref. [2], a nonrelativistic expression was derived for calculating the neutrino emissivity of the N-DURCA process. In 2001, a relativistic expression was presented in Ref. [52, 53]. As the EOSs adopted in the present work were calculated from relativistic theories, we thus self-consistently employed the relativistic expression to calculate the neutrino emissivity. The relativistic expression is given by

$$\begin{aligned}Q_{\mathrm{R}} = &\frac{450\pi}{10080}G_{\mathrm{F}}^2C^2T^6[f_1g_1((\varepsilon_{\mathrm{B}_1}+\varepsilon_{\mathrm{B}_2})p_{\mathrm{l}}^2\\ &-(\varepsilon_{\mathrm{B}_1}-\varepsilon_{\mathrm{B}_2})(p_{\mathrm{B}_1}^2-p_{\mathrm{B}_2}^2))+2g_1^2\mu_{\mathrm{l}}M_{\mathrm{B}_1}^*M_{\mathrm{B}_2}^*\\ &+(f_1^2+g_1^2)(\mu_{\mathrm{l}}(2\varepsilon_{\mathrm{B}_1}\varepsilon_{\mathrm{B}_2}-M_{\mathrm{B}_1}^*M_{\mathrm{B}_2}^*)+\varepsilon_{\mathrm{B}_1}p_{\mathrm{l}}^2\\ &-\frac{1}{2}(\varepsilon_{\mathrm{B}_1}+\varepsilon_{\mathrm{B}_2})(p_{\mathrm{B}_1}^2-p_{\mathrm{B}_2}^2+p_l^2))]\Theta(p_{\mathrm{l}}^2+p_{\mathrm{B}_2}^2-p_{\mathrm{B}_1}^2),\end{aligned} \tag{5}$$

where $G_{\mathrm{F}}=1.436\times10^{-49}$ erg cm^3 is the weak coupling constant; $C=\cos\theta_{\mathrm{c}}(\sin\theta_{\mathrm{c}})=0.973(0.231)$ for a change of strangeness $|\Delta S|=0(1)$; T is the temperature; f_1 and g_1 are the vector and axial-vector coupling constants; μ_{l} and p_{l} are the chemical potential and Fermi momenta of leptons l; $\varepsilon_{\mathrm{B}_i}$, p_{B_i} and $M_{\mathrm{B}_i}^*$ are the kinetic energy, Fermi-momenta and effective mass of baryons B_i; and $\Theta(x)=1$ if $x\geqslant0$ and zero otherwise. The total neutrino emissivity in this paper is the sum of the electron and muon N-DURCA processes.

3 Results and discussion

3.1 Neutrino emissivity of rotational traditional neutron stars

The effects of rotation on the N-DURCA process using the MDI and APR EOSs for traditional neutron stars (composed of β-equilibrium nuclear matter) were studied in Refs. [16] and [17] respectively. They suggested that the proton fraction could drop below x_{DU} with increasing rotational frequency, and thus make the N-DURCA process impossible. However, they only studied mass sequences whose proton fractions are close to x_{DU}.

We adopted the effective interactions from the RMF and CQMC theories to calculate the EOSs and employed the RNS code to simulate rotational traditional neutron stars. The calculated results are shown in Fig. 3, including the particle density (ρ_{c}), proton fraction (X_{p}), electron fraction (X_{e}), muon fraction (X_{μ}), and total neutrino emissivity as a function of the rotational frequency (f) for PKDD and MYN EOSs. Four baryonic mass sequences of neutron star from 0.9 to 2.1 $M_{\odot}$ have been fixed. The horizontal dashed lines in (b) represent x_{DU} for PKDD and MYN EOSs, respectively. As shown in Fig. 3, all ρ_{c}, X_{p}, X_{e} and X_{μ} decrease with increasing rotational frequency for a fixed baryonic mass sequence. In addition, we can see from Fig. 3(b) that X_{p} for 1.3 $\sim$ 1.7 $M_{\odot}$ of the MYN EOS can drop below x_{DU}, and thus the N-DURCA process becomes impossible, which is consistent with the results suggested by Refs. [16] and [17]. Similarly, the N-DURCA process can become impossible for 0.9 $\sim$ 1.3 $M_{\odot}$ of the PKDD EOS with the rotational frequency increase.

To study the mass dependence of neutrino emissivity for traditional neutron stars, the total neutrino emissivity of several mass sequences has been calculated and the results are presented in Fig. 3(e). As shown in Fig. 3(e), the neutrino emissivity is nearly invariable with increasing rotational frequency for a fixed baryonic mass sequence and the maximum change of neutrino emissivity is 5%, 5% (0.8%) and 2% (3%) for 1.3, 1.7 and 2.1 $M_{\odot}$ respectively of the PKDD (MYN) EOS, if the break of 2.1 $M_{\odot}$ is ignored. The break appears due to the muon N-DURCA process being forbidden at 794 (996) Hz and only the electron N-DURCA process existing at higher frequencies for the PKDD (MYN) EOS. ρ_{c} decreases with increasing f as shown in Fig. 3(a), while the corresponding neutrino emissivity changes little, which indicates the neutrino emissivity is not determined simply by the particle fractions.

To study the EOS dependence of neutrino emissivity for traditional neutron stars, the total neutrino emissivity as a function of the rotational frequency for RMF and CQMC EOSs without hyperons is presented in Fig. 5(a). The baryonic mass sequence is fixed as 1.6 $M_{\odot}$ for all the EOSs. We can see from Fig. 5 that the neutrino emissivity is invariable with increasing rotational frequency for all the EOSs.

Based on the present calculations, though the rotation obviously changes the particle fractions of neutron stars, the neutrino emissivity is nearly invariable for traditional neutron stars with a fixed baryonic mass, which is independent of the EOSs and the mass of the star.

3.2 Neutrino emissivity of the rotational hyperonic neutron star

As mentioned above, hyperons could suppress the neutrino emissivity of the N-DURCA process while rotation has no apparent effect on it. However, for a rotational hyperonic neutron star (including strangeness bearing baryons), the effects of hyperons and rotation on the N-DURCA process must be considered simultaneously.

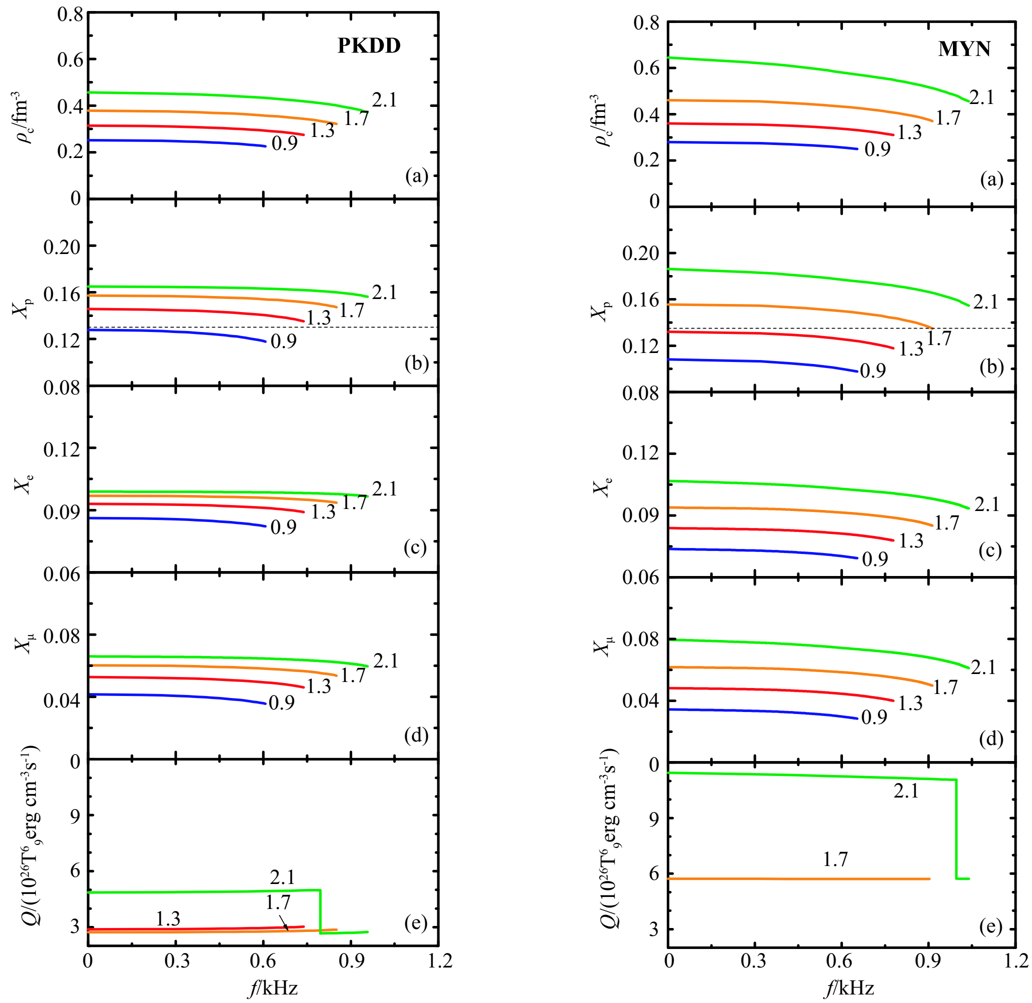

Fig. 3. (color online) The central particle density (ρ_c), proton fraction (X_p), electron fraction (X_e), muon fraction (X_μ), and neutrino emissivity (Q) as a function of the rotational frequency (f) for PKDD and MYN EOSs. Four baryonic mass sequences of neutron stars from 0.9 to 2.1 $M_\odot$ are selected. The horizontal dashed lines in (b) represent x_{DU} for PK1 and MYN EOSs. All lines start at the static limit and end at the Keplerian limit.

In order to study the effects, we adopted the effective interactions from the RMF and CQMC theories to calculate the EOSs with hyperons and employed the RNS code to simulate rotational hyperonic neutron stars. The calculated results of several baryonic mass sequences of neutron stars involving hyperons are given in Fig. 4. The baryonic mass sequences are selected from 1.2 $M_\odot$(2.0 $M_\odot$) where hyperons appear, to the maximum baryonic mass sequence for the PKDDH (MYNH) EOS. It can be seen in Fig. 4(a) that ρ_c still decreases with increasing f for a fixed baryonic mass sequence. As shown in Fig. 4(b), X_p decreases with increasing f for the selected mass sequences, except for the results for 2.2 $M_\odot$ of the PKDDH EOS. These tendencies can be understood by the relationship of $X_p\sim\rho$ in Fig. 2(a). For the PKDDH EOS, X_p increases with increasing ρ up to ρ= 0.55 fm^{-3} and then X_p decreases. As ρ_c of 2.2 $M_\odot$ is larger than 0.55 fm^{-3}, the relationship of $X_p\sim f$ exhibits the opposite behavior to the others. In Figs. 4 (c) and (d), both the relationships of $X_e\sim f$ and $X_\mu\sim f$ can be understood by $X_i\sim\rho$ in Fig. 2 in the same way.

To study the mass dependence of neutrino emissivity for hyperonic neutron stars, the neutrino emissivity of the N-DURCA process as a function of the rotational frequency (f) for the PKDDH and MYNH EOSs is presented in Fig.4(e). It is interesting to find that the neutrino emissivity of a rotational hyperonic neutron star increases with increasing f for all the mass sequences, no matter whether X_p increases or decreases. To be more precise, the neutrino emissivity increases by about 11%, 69%, 196% for 1.2, 1.7, 2.2 $M_\odot$ respectively of the PKDDH EOS, and 9%, 21%, 32% for 2.0, 2.1, 2.2 $M_\odot$

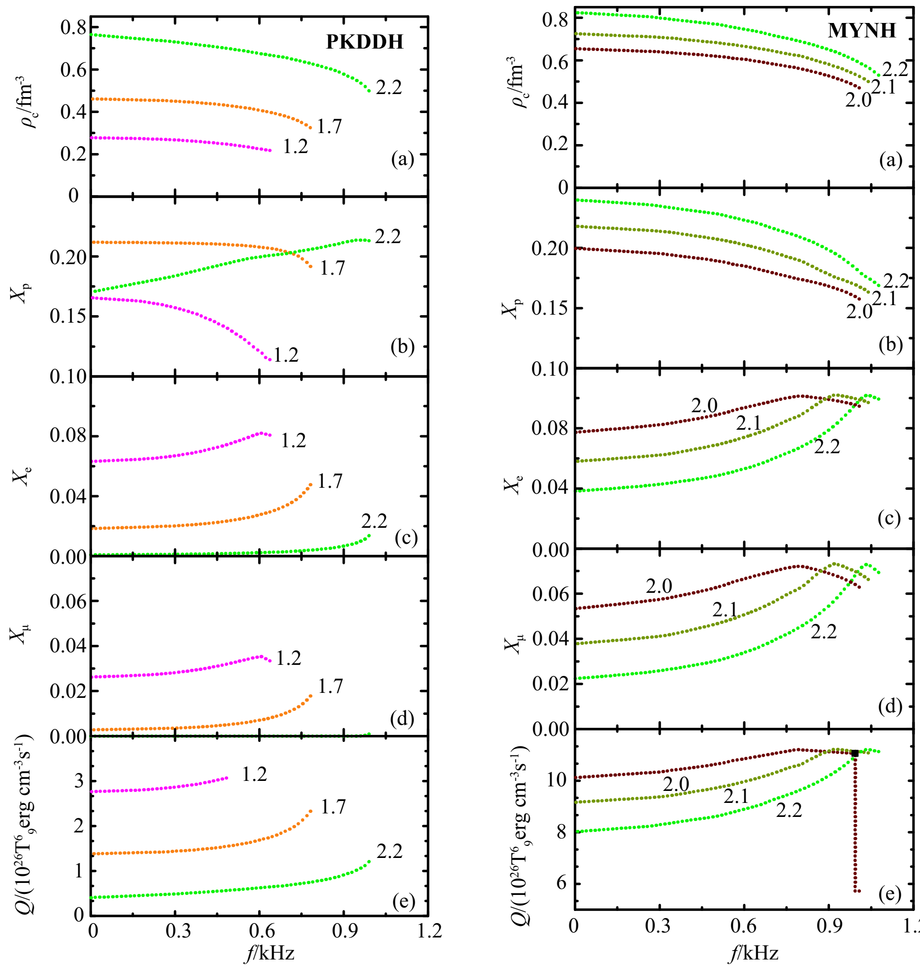

Fig. 4. (color online) Similar to Fig. 3 but for the PKDDH and MYNH EOSs. 1.2 and 2.0 $M_{\odot}$ are the mass sequences where hyperons just appear for these two EOSs, and 2.2 $M_{\odot}$ is the maximum baryonic mass sequence.

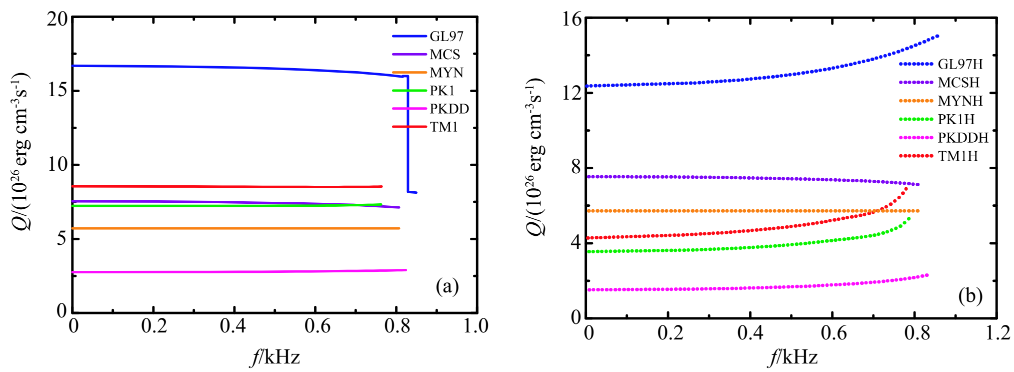

Fig. 5. (color online) The neutrino emissivity (Q) as a function of the rotational frequency (f) for the RMF and CQMC EOSs without (a) and with (b) hyperons. The baryonic mass sequence is fixed as 1.6 $M_{\odot}$ for all the EOSs.

respectively of the MYNH EOS. It is shown clearly that the neutrino emissivity increases with increasing f for all the mass sequences. The decrease of neutrino emissivity can be attributed to the overall effects of the terms needed in Eq. (5), including the Fermi momentum and chemical potential of leptons, Fermi momentum, effective mass and kinetic energy of the proton and neutron.

To study the EOS dependence of neutrino emissivity for hyperonic neutron stars, the total neutrino emissivity as a function of the rotational frequency for the RMF and CQMC EOSs with hyperons is presented in Fig. 5(b). The baryonic mass sequence is fixed as 1.6 $M_{\odot}$ for all the EOSs. We can see that the neutrino emissivity of all the EOSs increases with increasing rotational frequency, except for the MYNH and MCSH EOSs, because no hyperons exist in a neutron star with 1.6 $M_\odot$ constructed by these two EOSs. Thus, the neutrino emissivity increases with increasing rotational frequency for all the EOSs with the existence of hyperons.

In short, our calculated results indicate that the neutrino emissivity of the N-DURCA process can increase with increasing rotational frequency for a rotational hyperonic neutron star, which is different from the invariant tendency of a rotational traditional neutron star given in Fig 3(e). Thus, the effects of rotation on the N-DURCA process for traditional and hyperonic neutron stars are apparently different.

4 Summary

Based on the relativistic mean field model and chiral quark - meson coupling model, we have studied the effects of rotation on the N-DURCA process of neutron stars. The neutrino emissivity of rotational neutron stars has been calculated for the first time. We find that, for a fixed baryonic mass sequence of a traditional neutron star, the rotation may make the N-DURCA process impossible, which is consistent with the results suggested by Refs. [16] and [17]. Our present work further indicates that the neutrino emissivity is nearly independent of the rotational frequency for a traditional neutron star. For a fixed baryonic mass sequence of rotational hyperonic neutron stars, the neutrino emissivity of the N-DURCA process can increase with the frequency increase. The effects of rotation on the N-DURCA process for traditional and hyperonic neutron stars are apparently different, which is a possible way to analyze the internal composition of neutron stars.

The authors express their sincere gratitude to Dr. Miyatsu and Prof. Saito for providing the MYN and MCS EOSs.

References

1 S. L. Shapiro, & S. A. Teukolsky, *Black Holes, White Dwarfs, and Neutron Stars: The Physics of Compact Objects* (New York: A Wiley-Interscience Publication, 1983)
2 J. M. Lattimer, C. J. Pethick, M. Prakash, and P. Haensel, Phys. Rev. Lett., **66**: 21 (1991)
3 D. G. Yakovlev, O. Y. Gnedin, A. D. Kaminker, and A. Y. Potekhin, AIP Conf. Proc., **983**: 379 (2008)
4 D. Page, U. Geppert, and F. Weber, Nucl. Phys. A, **777**: 497 (2006)
5 D. G. Yakovlev, A. D. Kaminkera, O. Y. Gnedinc, and P. Haenseld, Physics Reports, **354**: 1 (2001)
6 N. K. Glendenning, Astrophys. J., **293**: 470 (1985)
7 W. B. Ding, Z. Yu, and Y. H. Liu, Chin. Phys. Lett., **28**: 072601 (2011)
8 Y. Xu, G. Z. Liu, Y. R. Wu, M. F. Zhu, Z. Yu, H. Y. Wang, and E. G. Zhao, Chin. Phys. Lett., **28**: 079701 (2011)
9 Y. Xu, G. Z. Liu, C. Z. Liu, C. B. Fan, H. Y. Wang, M. F. Zhu, and E. G. Zhao, Chin. Phys. Lett., **30**: 129501 (2013)
10 Y. Xu, G. Z. Liu, C. Z. Liu, C. B. Fan, X. W. Han, X. J. Zhang, H. Y. Wang, M. F. Zhu, and Y. Meng, Chin. Sci. Bull., **59**: 273 (2014)
11 Y. Xu, X. L. Huang, X. J. Zhang, T. Bao, L. Xiao, C. B. Fan, and C. Z, Liu, arXiv:1509.05150v4 (2016)
12 M. Prakash, M. Prakash, J. M. Lattimer, and C. J. Pethick, Astrophys. J., **390**: L77 (1992)
13 C. Schaab, S. Balberg, and J. Schaffner-Bielich, Astrophys. J., **504**: L99 (1998)
14 D. Page, M. Prakash, J. M. Lattimer, and A. Steiner, Phys. Rev. Lett., **85**: 2048 (2000)
15 I. Vidana and L. Tolos, Phys. Rev. C, **70**: 028802 (2004)
16 P. G. Krastev, B. A. Li, and A. Worley, Astrophys. J., **676**: 1170 (2008)
17 R. Negreiros, S. Schramm, and F. Weber, Astron. Nachr., **335**: 703 (2014)
18 J. Meng, H. Toki, S. G. Zhou, S. Q. Zhang, W. H. Long, and L. S. Geng, Prog. Part. Nucl. Phys., **57**: 470 (2006)
19 P. Ring, Prog. Part. Nucl. Phys., **37**: 193 (1996)
20 S. F. Ban, J. Li, S. Q. Zhang, H. Y. Jia, J. P. Sang, and J. Meng, Phys. Rev. C, **69**: 045805 (2004)
21 N. B. Zhang, B. Qi, S. Y. Wang, S. L. Ge, and B. Y. Sun, Int. Jou. Mod. Phys. E, **22**: 1350085 (2013)
22 C. Y. Ryua, M. K. Cheouna, T. Kajinob, T. Maruyamad, and G. J. Mathewse, Astroparticle Physics, **38**: 25 (2012)
23 T. Miyatsu, S. Yamamuro, and K. Nakazato, Astrophys. J., **774**: 4 (2013)
24 J. N. Hu, A. Li, H. Toki, and W. Zuo, Phys. Rev. C, **89**: 025802 (2014)
25 H. Fujii, T. Maruyama, T. Muto, and T. Tatsumi, Nucl. Phys. A, **597**: 645 (1996)
26 N. K. Glendenning, and J. Schaffner-Bielich, Phys. Rev. Lett., **81**: 4564 (1998)
27 W. Z. Jiang, B. A. Li, and L. W. Chen, Astrophys. J., **756**: 56 (2012)
28 D. B. Kaplan, and A. E. Nelson, Phys. Lett. B, **175**: 57 (1986)
29 B. Y. Sun, W. H. Long, J. Meng, and U. Lombardo, Phys. Rev. C, **78**: 065805 (2008)
30 S. Wang, H. F. Zhang, and J. M. Dong, Phys. Rev. C, **90**: 055801 (2014)
31 B. Qi, N. B. Zhang, S. Y. Wang, and B. Y. Sun, Chin. Phys. Lett., **32**: 112101 (2015)
32 B. Qi, N. B. Zhang, B. Y. Sun, S. Y. Wang, and J. H. Gao, RAA, **16**: 60 (2016)
33 T. Miyatsu, M. K. Cheoun, and K. Saito, Phys. Rev. C, **88**: 015802 (2013)
34 P. A. M. Guichon, Phys. Lett. B, **200**: 235 (1988)
35 K. Saito, and A. W. Thomas, Phys. Lett. B, **327**: 9 (1994)
36 P. A. M. Guichon, A. W. Thomas, and K. Tsushima, Nucl. Phys. A, **814**: 66 (2008)
37 T. Miyatsu, and K. Saito, PThPh, **122**: 1035 (2010)
38 S. Nagai, T. Miyatsu, K. Saito, and K. Tsushima, Phys. Lett. B, **666**: 239 (2008)
39 N. K. Glendenning, *Compact Stars, Nuclear Physics, Particle-Physics and General Relativity*, 2nd ed. (Springer-Verlag, New York, 2000)
40 W. H. Long, J. Meng, N. Van Giai, and S. G. Zhou, Phys. Rev. C, **69**: 034319 (2004)
41 Y. Sugahara, and H. Toki, Prog. Theor. Phys., **92**: 803 (1994)
42 S. A. Moszkowski, Phys. Rev. D, **9**: 1613 (1974)

43 J. W. Negele, and D. Vautherin, Nucl. Phys. A, **207**: 298 (1973)
44 G. Baym, C. Pethick, and D. Sutherland, Astrophys. J., **170**: 299 (1971)
45 J. Rikovska-Stone, G P. A. M. uichon, H. H. Matevosyan, and A. W. Thomas, Nucl. Phys. A, **792**: 341 (2007)
46 D. L. Whittenbury, J. D. Carroll, A. W. Thomas, K. Tsushima, and J. R. Stone, arXiv:1204.2614 (2012)
47 N. Stergioulas, Living Rev. Relativ., **6**: 3 (2003)
48 H. Komatsu, Y. Eriguchi, and I. Hachisu, MNRAS, **237**: 355 (1989)
49 G. B. Cook, S. L. Shapiro, and S. A. Teukolsky, Astrophys. J., **424**: 823 (1994)
50 N. Stergioulas, and J. L. Friedman, Astrophys. J., **444**: 306 (1995)
51 T. Nozawa, N. Stergioulas, E. Gourgoulhon, and Y. Eriguchi, A & A, **132**: 431 (1998)
52 L. B. Leinson, and A. Pérez, Phys. Lett. B, **518**: 15 (2001a)
53 L. B. Leinson, and A. Pérez, Phys. Lett. B, **522**: 358 (2001b)